Invited Paper

A Brief review on terahertz metamaterial perfect absorbers

Li Huang [1] and Hou-Tong Chen [2*]
[1] Physics Department, Harbin Institute of Technology, Harbin, Heilongjiang 150001, China
[2] Center for Integrated Nanotechnologies, Los Alamos National Laboratory, Los Alamos, New Mexico 87545, USA
[1] Email: lihuang2002@hit.edu.cn
[*2] Email: chenht@lanl.gov

(Received January 2, 2013)

Abstract: Metal-dielectric-metal metamaterial structures have enabled near-unity absorption with deep sub-wavelength thickness. The high absorption and low mass volume, as well as the structure simplicity, compactness and design flexibility, are important for many potential applications. They have attracted great worldwide interest in the whole electromagnetic spectrum range, and may have special significance in the terahertz regime. This paper provides a brief review on the development of terahertz metamaterial perfect absorbers, particularly focusing on the design principle, thickness reduction, bandwidth broadening, and theoretical modelling.

Keywords: Metamaterials, Terahertz, Absorbing materials, Interference, Electromagnetic waves

doi: 10.11906/TST.026-039.2013.03.02

1. Introduction

Metamaterials [1, 2] are a new class of artificially structured effective media exhibiting exotic properties and enabling emergent phenomena which are impossible or very difficult to realize using naturally occurring materials. They are best represented by negative index of refraction [1, 3], super-resolution optical imaging circumventing diffraction limits [4, 5], and electromagnetic cloaking and transformation optics [6-8]. During the past decade, metamaterial research has evolved from microwave [3] to terahertz (THz) [9, 10] and optical [11-13] frequencies, from passive to active [14], from linear to nonlinear [15-17], from classical to quantum [18], and from metamaterials to metadevices [19-21].

Metamaterials research is of special significance in solving the material issues encountered in the THz frequency regime [22]. The far infrared or THz is considered one of the least developed frequency regimes in the electromagnetic spectrum, though it is very attractive for numerous promising applications [23, 24]. This “THz gap” is essentially due to the lack of both classical electronic response (present for microwave and lower frequencies) and quantum photonic response (present for infrared and higher frequencies) in the THz frequency range. A designed and controllable metamaterial resonant response, both passive and active, or linear and nonlinear, would dramatically enhance the interactions between THz radiation and materials. It becomes the foundation for further development of many THz devices and components achieving novel functionalities and unprecedented performance, a new opportunity that would not be possible using solely naturally existing materials [22].

Among many metamaterial functionalities is the accomplishment of near-unity absorption [25]. Perfect absorption is essentially a problem of impedance matching to free space. However, natural materials rarely possess such electromagnetic properties to accomplish impedance matching $Z = \sqrt{\mu(\omega)/\varepsilon(\omega)} = Z_0$, where $\mu(\omega)$ and $\varepsilon(\omega)$ are the magnetic permeability and electric permittivity of the material, respectively, and Z_0 is the free space impedance. The design flexibility of metamaterials provides an excellent opportunity to achieve perfect absorption through minimizing the reflection [26] and simultaneously eliminating the transmission using specifically designed metallic structure whose thickness is much smaller than the operational wavelength. Metamaterial perfect absorbers are attractive in many applications such as imaging [27, 28], selective thermal emitters [29], sensors [30], thin-film solar harvesting [31, 32], and cloaking devices [33, 34]. While metamaterial perfect absorbers are scalable to operate at almost any relevant electromagnetic spectrum [35], in this review paper, we largely limit our scope to the development of THz metamaterial perfect absorbers.

2. Metamaterial perfect absorbers

2.1 Classical electromagnetic absorbers

Perfect absorption becomes possible only when the reflection at an interface can be completely eliminated. As it is difficult to match the impedance between free space and an absorbing material, classical electromagnetic absorbers typically employ an alternative approach by taking advantage of multireflection and interference. For example, a Salisbury screen [36] as shown in Fig. 1(a) consists of a thin resistive layer and a metal ground plane separated by a dielectric spacer with a quarter-wavelength thickness, by which the direct and following reflections can be equal in magnitude but out of phase, resulting in a destructive interference and cancellation of reflection. The incident electromagnetic wave is therefore completely trapped in the structure and dissipated in the resistive screen. However, the drawbacks of Salisbury screens are also obvious: they are bulky and operate over a narrow bandwidth, restricting their use in many applications. Broadening the bandwidth can be accomplished by using multilayered structures, forming the so-called Jaumann absorbers [36]. In circuit analog absorbers [36], the top sheet not only contains a resistive component but is also reactive, by using frequency selective surfaces loaded with loss. The design however still requires a dielectric spacer of approximately a quarter-wavelength thickness.

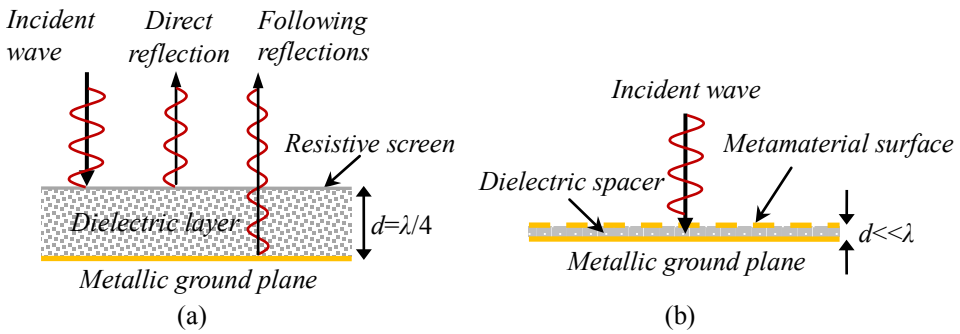

Fig. 1 Sketches of a Salisbury screen (a) and a metamaterial perfect absorber (b).

2.2 Metamaterial perfect absorbers

In classical electromagnetic absorbers, the reflection from the low-impedance ground plane gives a phase shift of π and the quarter-wavelength thick dielectric layer provides an additional propagation phase of π. The total phase change within a round-trip propagation path is then 2π (or zero), satisfying the phase matching condition for constructive interference during the multireflection process and destructive interference with the direct reflection. If we can convert the low-impedance ground plane (electric conductor) to a high-impedance ground plane (magnetic conductor) by adding a metamaterial surface above the ground plane separated with a thin dielectric layer, as suggested by Engheta [37], the overall absorber thickness can be dramatically reduced. Interestingly, such a metamaterial structure as shown in Fig. 1(b) itself can serve as a perfect absorber, when we take into account losses in the metal and dielectric materials, and employ appropriate metamaterial structures and thickness of the dielectric spacer.

The first metamaterial perfect absorber was demonstrated in the microwave frequency range by Landy *et al.* [25]. The unit cell consists of an electric split-ring resonator (eSRR) and a cut-wire (CW) with a thin dielectric spacer between them, as schematically shown in Fig. 2(a). Reflectance $R(\omega)$ and transmittance $T(\omega)$ of the structure were simulated and experimentally measured, and the absorption was given by $A(\omega) = 1 - R(\omega) - T(\omega)$. It was shown that $R(\omega)$ and $T(\omega)$ could reach nearly zero simultaneously at about 11.5 *GHz*, thereby accomplishing near-unity absorption. The simulated absorption $A(\omega) = 96\%$ was in good agreement with the experimentally measured value of 88%. It was also shown that the absorption decreases rapidly with increasing incident angles, and the full-range of incident angle was measured to be 16° with $A(\omega) > 0.5$. Obviously, this metamaterial perfect absorber is polarization sensitive.

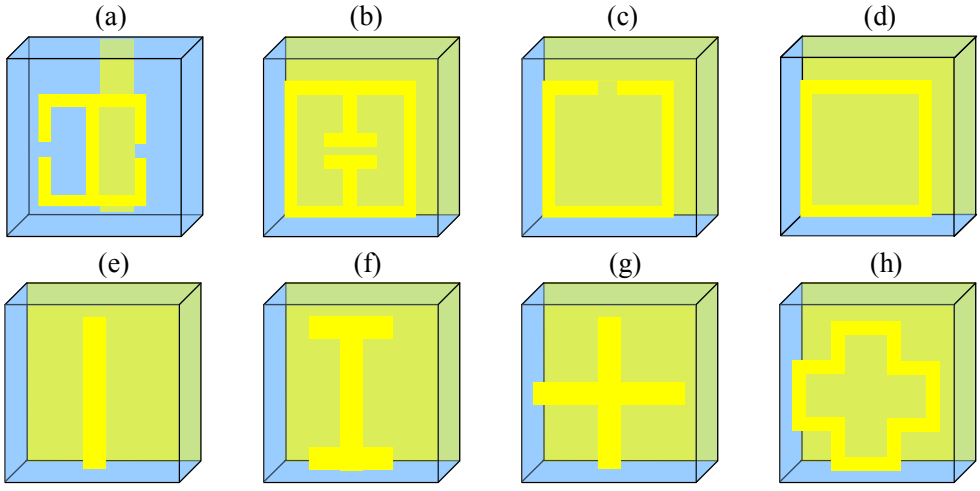

Fig. 2 Typical unit cells adopted in narrowband metamaterial perfect absorbers.

2.2 Terahertz metamaterial perfect absorbers

The design of metamaterial perfect absorbers [25] was soon translated to the THz frequency

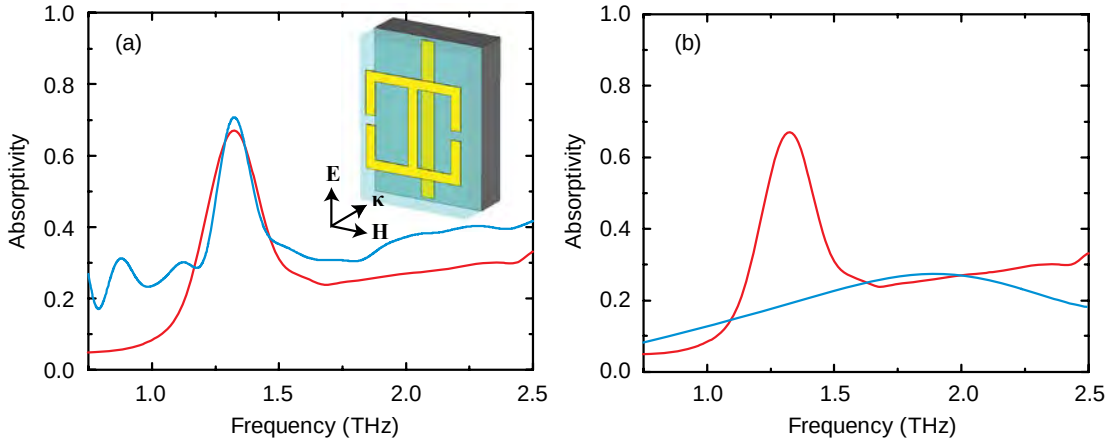

Fig. 3 (a) Experimentally measured (blue) and numerically simulated (red) absorptivity for the THz metamaterial absorber unit structure shown in the inset. (b) Absorptivity for the structure when the incident electric field is parallel (red) and perpendicular (blue) to the cut-wire. Figures reproduced with permission from ref. 38. Copyright OSA.

range by scaling [38]. With the incident polarization shown in the inset to Fig. 3(a), the experimentally measured absorptivity reaches 70%, in good agreement with the simulated value of 68%. This metamaterial absorber operates at 1.3 *THz* with a 6 μm thick polyimide spacer, which is 1/40 of the free space wavelength. It should be noted that the spacer thickness plays an important role in accomplishing best absorption performance. When the incident electric field is perpendicular to the center stalk of the eSRR, the simulated absorptivity is only 27% as shown in Fig. 3(b). The polarization dependence of absorption is directly due to the two-fold rotation symmetry of the metamaterial structure. For polarization independent THz metamaterial perfect absorbers, it is necessary to design metamaterial structures containing four-fold rotation symmetry [39-43], such as those shown in Fig. 2(d, g, h).

It was demonstrated soon after that the CW array in Refs. [25, 38] could be replaced by a metal ground plane [44, 45], making the metamaterial perfect absorbers similar to circuit analog

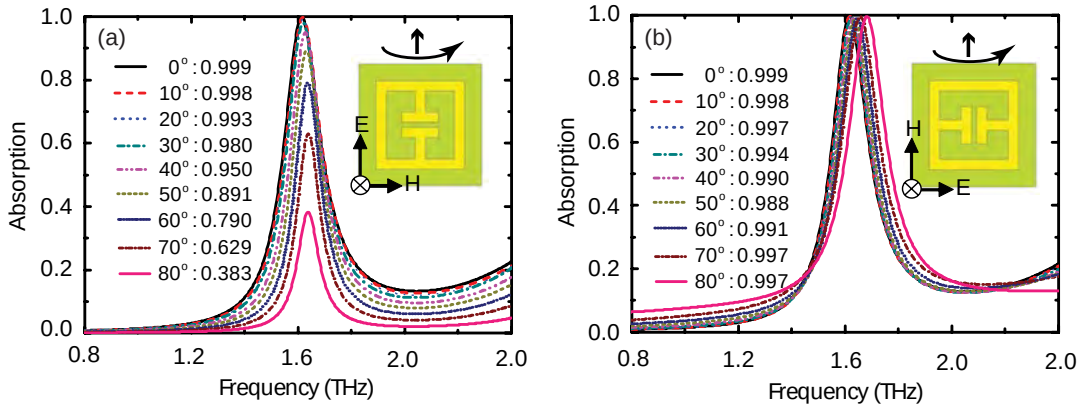

Fig. 4 Numerically simulated absorptivity under various incidence angles for TE (a) and TM (b) polarizations. Figures reproduced with permission from ref. 44. Copyright APS.

absorbers [36] but with a much thinner spacer thickness. The use of a continuous ground plane simplifies the sample fabrication process. Furthermore, it prevents the incident electromagnetic waves from transmitting through, so only reflection measurements are necessary as $T(\omega) = 0$ implies $A(\omega) = 1 - R(\omega)$. Many metamaterial structures have been employed to make narrowband absorbers, including SRRs, CWs, and frequency selective surface (FSS) elements, with a few typical ones shown in Fig. 2. They are either polarization dependent [Fig. 2 (a-c, e, f)] or independent [Fig. 2(d, g, h)]. It was shown that the use of a ground plane enables wide-angle operation [40, 44, 45]. As shown in Fig. 4, the metamaterial absorber is capable of near-unity absorption at all incident angles ranging from 0° to 80° for TM polarization, whereas the absorptivity decreases rapidly when the incident angle is above 40° for TE polarization [40, 44].

2.3 Multiband and broadband THz metamaterial perfect absorbers

There are mainly two approaches to expand the narrowband absorption into multiband or broadband operation. One way is to combine two or more resonators with different sizes forming a super-unit-cell, and the other way is to stack multiple layers of resonators with different geometric dimensions separated by dielectric layers with appropriate thicknesses.

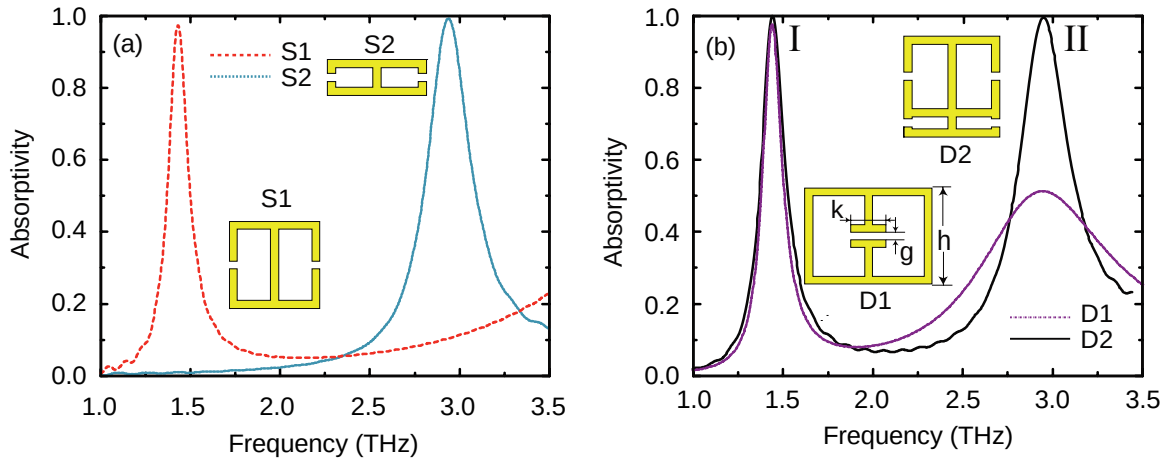

Fig. 5 Dual-band THz metamaterial perfect absorbers. Figures reproduced with permission from ref. 47. Copyright IOP.

The individual metamaterial structures with different geometric dimensions, eSRRs S1 and S2 shown in the insets to Fig. 5 (a), can be used to realize metamaterial absorbers operating at different frequencies, with the absorption spectra shown in Fig. 5(a). When S1 and S2 are combined together forming a new dual-band resonator [46], shown as D2 in the inset to Fig. 5(b), the resulted metamaterial absorber exhibits dual absorption peaks corresponding to the spectral superposition of S1 and S2 [47], as shown in Fig. 5(b). It turns out that the multiple resonances in a metamaterial element can be used to realize a multiband metamaterial absorber [e.g. D1 in Fig. 5(b)]. A similar design [48] was demonstrated by Wen *et al*. More dual-band and multiband metamaterial perfect absorbers in the THz frequency regime have been demonstrated, mostly

using a super-unit-cell containing several metamaterial elements resonating at distinct frequencies [42, 49].

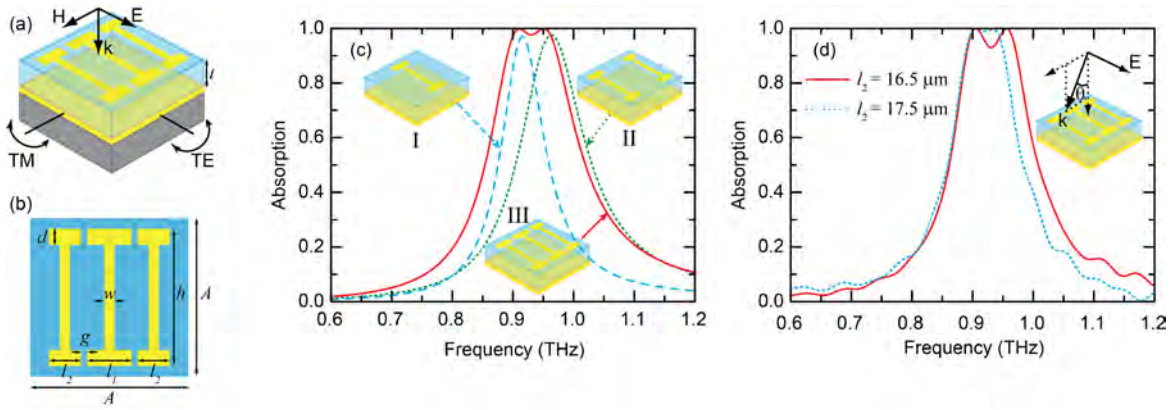

Fig. 6 (a) Schematic and (b) top view of a super-unit-cell for absorption bandwidth broadening. (c) Simulated absorption spectra at normal incidence with three different configurations I, II, and III, which are indicated in the insets. (d) Experimental absorption spectra of two metamaterial absorbers in configuration III with slightly different end loading of side I-shaped resonator, l_2 = 16.5 μm or 17.5 μm.

Expanding the bandwidth around a specific frequency can be accomplished by using resonators in a super-unit-cell with close resonance frequencies. For such a purpose, we used two sets of I-shaped resonators in the super-unit-cell shown in Fig. 6(a, b). As shown in Fig. 6(c), the center I-shaped resonator (Configuration I) and the two identical side I-shaped resonators (Configuration II) exhibit distinct but close peak absorption frequencies. Combining them

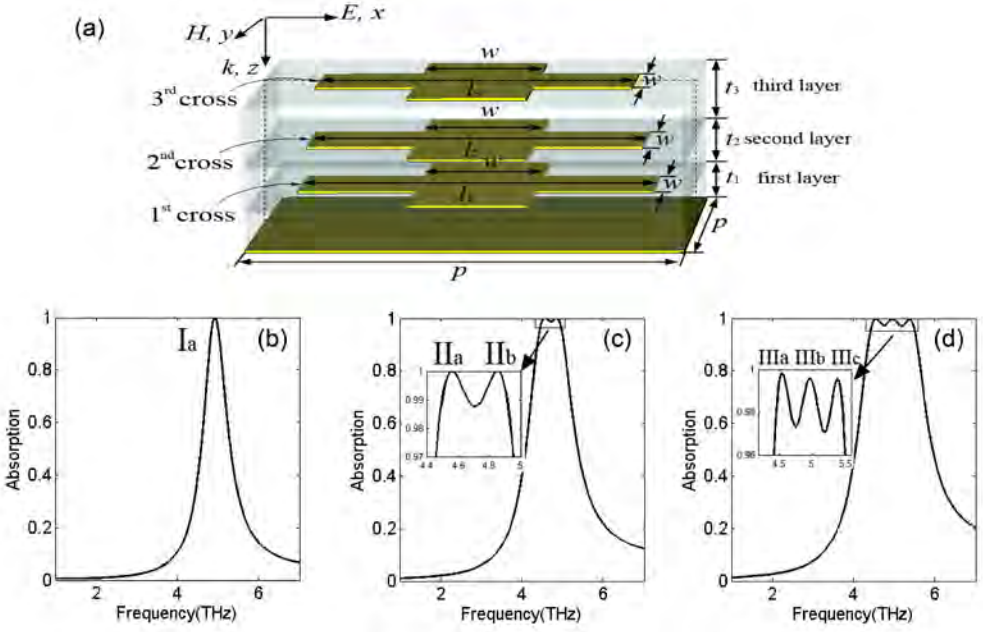

Fig. 7 (a) Schematic of a metamaterial absorber unit cell consisting of three layers of cross-resonators. (b)-(d) Simulated absorption spectra for one-layer, two-layer, and three-layer cross-resonator absorbers. Courtesy of Y. Q. Ye and with permission. Copyright OSA.

together into a super-unit-cell (Configuration III) results in a superposition of the absorption spectra [50], shown in Fig. 6(c). The bandwidth of the absorption is effectively broadened as compared to the individual ones. The flatness of the absorption top is improved using closer resonance frequencies, but with the price of a slightly narrower bandwidth, as shown in Fig. 6(d). Broadband THz absorption can also be achieved by simply stacking several layers of resonators with different geometric dimensions and appropriate spacer thicknesses [51, 52]. Figure 7(a) illustrates a metamaterial absorber structure consisting of three layers of cross-resonators. The absorption bandwidth is significantly improved with increasing layers of cross-resonators with appropriate geometric dimensions and spacer thicknesses, as shown in Fig. 7(b-d). The design of this kind of metamaterial perfect absorbers is quite similar to the classical Jaumann absorbers [36] for bandwidth broadening.

3. Modeling metamaterial perfect absorbers

3.1 Bulk effective medium model

The majority of works on metamaterial perfect absorbers follow the concept of bulk effective medium as it was used to explain the impedance matching at the very beginning [25, 38]. This theory considers the metamaterial absorber as an effective medium characterized by electric permittivity $\varepsilon(\omega)$ and magnetic permeability $\mu(\omega)$. The permittivity is attributed to the electric resonant response of individual metamaterial elements, and the permeability is due to the magnetic resonance resulting from anti-parallel surface currents between the two layers of metallic metamaterial structures or between the top metamaterial element and the ground plane [25, 38, 44]. They can be independently tailored through adjusting the geometric dimensions of the metamaterial resonators and the spacer thickness. In such a way, impedance matching to free space becomes possible, i.e., $Z = \sqrt{\mu(\omega)/\varepsilon(\omega)} = Z_0$ can be satisfied at a specific frequency. Consequently, there is no reflection and the incident electromagnetic wave is completely absorbed in the metamaterial structure as the metal and the dielectric spacer are essentially lossy.

Note that effective medium theory is based on the assumption that the metamaterial absorber is homogeneous. However, even for a freestanding metamaterial absorber, the structure is highly asymmetric in the wave propagation direction. The metamaterial structure can completely absorb the electromagnetic wave that is incident from the front; it functions as a near-perfect reflector when the incident electromagnetic wave comes from the back. On the other hand, the excitation of anti-parallel surface currents was used as the direct evidence of a magnetic resonance [30, 38, 44]. However, it was shown that such anti-parallel surface currents can be directly derived from an interference model [53] where the metamaterial absorber was treated as a resonant cavity.

3.2 Interference model

In the interference model, the two metallic layers in a metamaterial absorber are treated as

zero-thickness impedance-tuned surfaces that dramatically modify the amplitude and phase of the reflection and transmission coefficients as compared to those for the original interfaces formed by the two bounding media. The metal-dielectric-metal metamaterial absorber thereby forms a cavity where multireflection occurs [26, 53], as shown in the inset to Fig. 8(c). The overall reflection is then the superposition of the direct reflection and the following multireflection. With

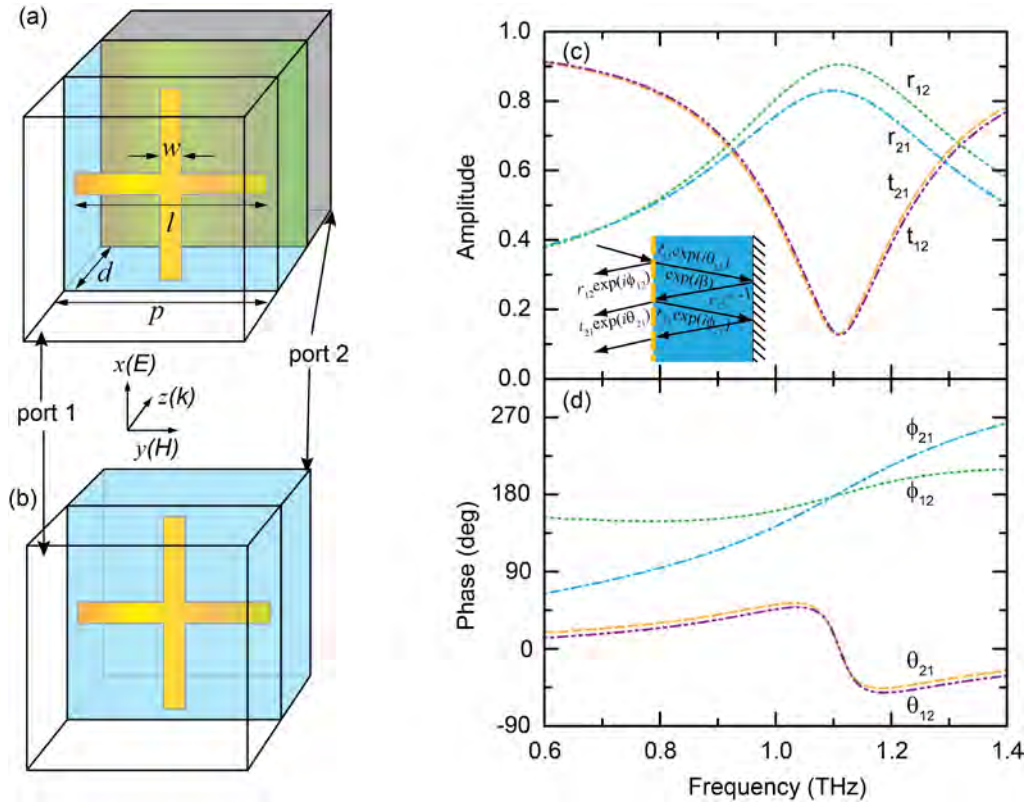

Fig. 8 (a) An example metamaterial absorber unit cell structure and (b) its isolated air-cross-spacer interface for numerical simulations. (c) Simulated amplitude and (d) phase of reflection and transmission coefficients at the air-cross-spacer interface. Inset: schematic of the multireflection and interference model.

appropriate design of the metamaterial structure, it is possible to achieve a completely destructive interference and cancellation of the reflection, similar to a classical Salisbury screen or quarter-wave antireflection coating. In other words, the incident electromagnetic wave is trapped in the metamaterial cavity and eventually dissipated, resulting in the near-unity absorption.

In an example metamaterial absorber schematically shown in Fig. 8(a), the incident electromagnetic wave is partially reflected (direct reflection) by the air-cross-spacer interface, and the rest is transmitted into the spacer. The latter then encounters the ground plane, which is a perfect reflector and gives a phase shift of π for the reflection. This process continues as shown in the inset to Fig. 8(c) and results in the following reflections. A completely destructive interference between the direct and following reflections requires magnitude and phase matching. So the reflection and transmission coefficients at the air-cross-spacer have to be tailored. In order to realize ultrathin metamaterial absorbers, it is necessary to obtain a phase shift of $\sim\pi$ for the

reflection at the air-cross-spacer interface, which can be accomplished due to its highly dispersive resonant response [53].

The reflection and transmission coefficients at the air-cross-spacer interface, denoted by r_{12}, t_{12}, r_{21}, and t_{21}, and their corresponding phase shifts φ_{12}, θ_{12}, φ_{21}, and θ_{21}, can be obtained through numerical simulations using the unit cell shown in Fig. 8(b). The results are shown in Fig. 8(c,d). The overall reflection with the presence of the ground plane is given by [26, 53]:

$$\tilde{r} = \tilde{r}_{12} - \frac{\tilde{t}_{12}\tilde{t}_{21}e^{i2\tilde{\beta}}}{1+\tilde{r}_{21}e^{i2\tilde{\beta}}}. \tag{1}$$

The absorption $A(\omega)$ is then obtained with $A(\omega) = 1 - R(\omega) = 1 - \left|\tilde{r}(\omega)\right|^2$. It was shown that the theoretically calculated absorption exhibits excellent agreement with experimentally measured and numerically simulated (the whole absorber structure was used) results, as shown in Fig. 9(d), and they exhibit the same spacer thickness dependence [26, 53]. Furthermore, theoretical calculations revealed the anti-parallel surface currents at the two interfaces, due to the

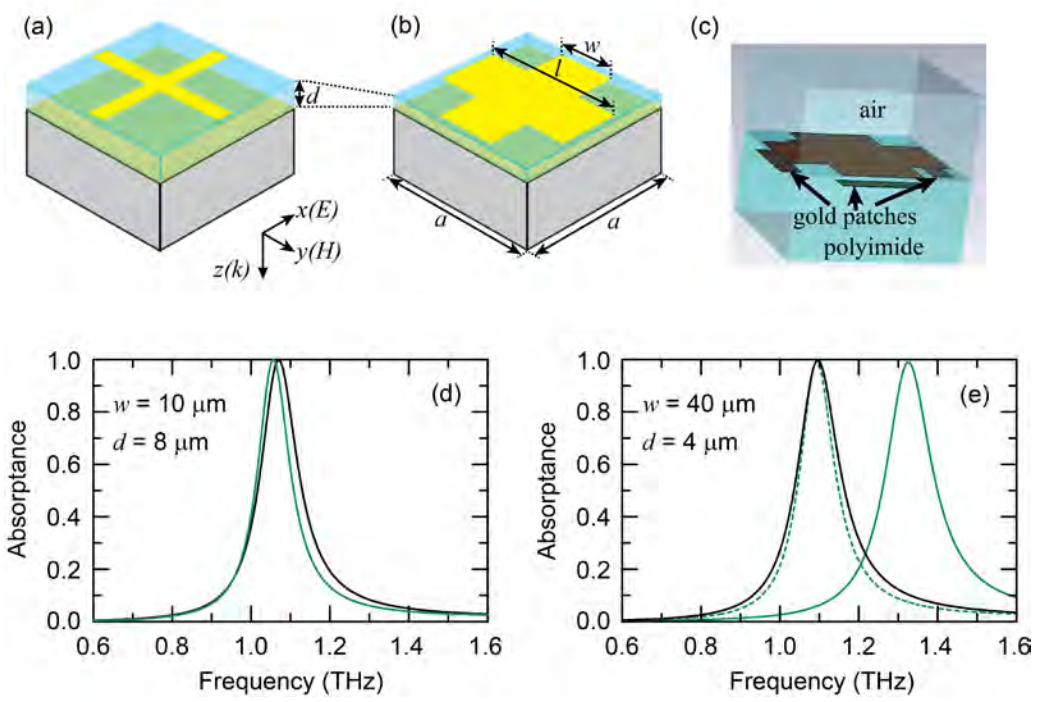

Fig. 9 (a) and (b) Increasing the width of the cross-resonator results in a reduced optimal spacer thickness. (c) Metal patches can be added at the position of ground plane to take into account the parasitic capacitance due to the near field interaction. (d) Numerically simulated (black) and theoretically calculated (green) absorption spectra for the metamaterial absorber with cross-resonator width $w = 10$ μm and spacer thickness $d = 8$ μm. (e) After increasing the cross-resonator width to $w = 40$ μm and reducing the spacer thickness to $d = 4$ μm, the numerically simulated (black solid) and theoretically calculated (green solid) absorption spectra show different peak frequency. After adding small patches in (c), the improved calculation (green dashed) shows good agreement.

interference and superposition [53] rather than a magnetic response excited by the incident magnetic field.

The simple interference model assumes that the near field coupling between the resonator array and the ground plane is negligible. However, this coupling might become significant particularly for an extremely thin spacer. It was demonstrated that the optimal spacer thickness decreases when the width of the cross-resonator increases, as shown in Fig. 9(b), and consequently the coupling becomes stronger [54]. In this case, as shown in Fig. 9(e), the theoretically calculated peak absorption frequency is significantly higher than the numerical simulations using the whole structure with cross-resonator width $w = 40$ μm and spacer thickness $d = 4$ μm. In order to take this strong coupling into account, we added four patches that are small but sufficient to cover the cross-resonator ends, to simulate the reflection and transmission coefficients of the air-cross-spacer interface [54], as shown in Fig. 9(c). These patches are embedded in the semi-infinite spacer and located at the ground plane position for the whole absorber structure. The improved theoretical calculations shown in Fig. 9(e) reveal excellent agreement with simulations. Further theoretical modeling shows that the coupling has to be also taken into account for the broadband THz metamaterial perfect absorbers [50].

3.3 Transmission line model

The transmission line model for metamaterial perfect absorbers is very similar to circuit analog absorbers, where the metamaterial structure is equivalent to an *RLC* circuit [55]. It assumes normal incidence and the coupling is negligible between the top eSRR and the bottom CW (or the ground plane) when considering the metamaterial perfect absorber structure illustrated in Fig. 2(a). Figure 10 shows the equivalent transmission line circuit [56]. The eSRR has two resonance modes, represented by R_1, L_1, C_1 and R_2, L_2, C_2, which couple to each other represented by M [55]. The CW was equivalent to the R_3, L_3 and C_3 circuit, and the spacer layer was treated as a propagating transmission line. The model calculations are in good agreement with numerical simulations [56]. In fact, in many aspects the transmission line model is equivalent to the interference model.

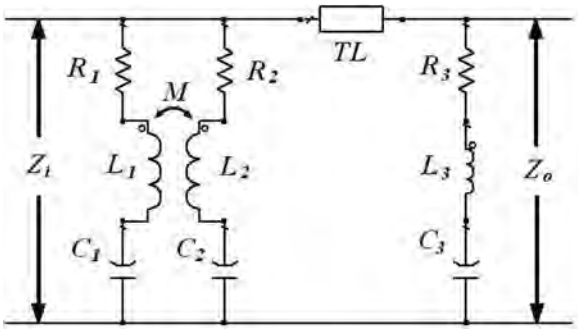

Fig. 10 Equivalent transmission line circuit model for the metamaterial perfect absorber structure shown in Fig. 2(a). Courtesy of Q. Y. Wen and with permission. Copyright OSA.

4. Conclusion and outlook

Much progress has been accomplished in the development and understanding of extremely thin THz metamaterial absorbers with very high absorption over wide-angle operation. These thin-film-like THz metamaterial perfect absorbers can be made freestanding and flexible, which makes them easily applicable to complex surfaces. Further effort is necessary to develop practical THz devices employing such exciting functionalities for various applications, e.g. THz sensing and imaging. Actively tunable and reconfigurable THz metamaterial perfect absorbers can be further accomplished through integration of active composite materials or devices into the building blocks, which may extend their practical usage.

L.H. acknowledges support from Natural Science Foundation of China (NSFC) under Grant No. 10904023. H.T.C. acknowledges partial support from the Los Alamos National Laboratory LDRD program. This work was performed, in part, at the Center for Integrated Nanotechnologies, a US Department of Energy, Office of Basic Energy Sciences Nanoscale Science Research Center operated jointly by Los Alamos and Sandia National Laboratories. Los Alamos National Laboratory, an affirmative action/equal opportunity employer, is operated by Los Alamos National Security, LLC, for the National Nuclear Security Administration of the US Department of Energy under contract DE-AC52-06NA25396.

References

[1] D. R. Smith, W. J. Padilla, D. C. Vier, et. al.. "Composite medium with simultaneously negative permeability and permittivity". *Phys. Rev. Lett.* 84, 4184-4187 (2000).

[2] V. M. Shalaev. "Optical negative-index metamaterials". *Nat. Photon.* 1, 41-48 (2007).

[3] R. A. Shelby, D. R. Smith, and S. Schultz. "Experimental verification of a negative index of refraction". *Science* 292, 77-79 (2001).

[4] J. B. Pendry. "Negative refraction makes a perfect lens". *Phys. Rev. Lett.* 85, 3966-3969 (2000).

[5] N. Fang, H. Lee, C. Sun, and X. Zhang. "Sub-diffraction-limited optical imaging with a silver superlens". *Science* 308, 534-537 (2005).

[6] J. B. Pendry, D. Schurig, and D. R. Smith. "Controlling electromagnetic fields". *Science* 312, 1780-1782 (2006).

[7] U. Leonhardt. "Optical conformal mapping". *Science* 312, 1777-1780 (2006).

[8] D. Schurig, J. J. Mock, B. J. Justice, et. al. "Metamaterial electromagnetic cloak at microwave frequencies". *Science* 314, 977-980 (2006).

[9] T. J. Yen, W. J. Padilla, N. Fang, et. al.. "Terahertz magnetic response from artificial materials". *Science* 303, 1494-1496 (2004).

[10] A. K. Azad, J. M. Dai, and W. L. Zhang. "Transmission properties of terahertz pulses through subwavelength

double split-ring resonators". *Opt. Lett.* 31, 634-636 (2006).

[11] S. Linden, C. Enkrich, M. Wegener, et. al. "Magnetic response of metamaterials at 100 terahertz". *Science* 306, 1351-1353 (2004).

[12] S. Zhang, W. J. Fan, N. C. Panoiu, et. al. "Experimental demonstration of near-infrared negative-index metamaterials". *Phys. Rev. Lett.* 95, 137404 (2005).

[13] V. M. Shalaev, W. S. Cai, U. K. Chettiar, et. al. "Negative index of refraction in optical metamaterials". *Opt. Lett.* 30, 3356-3358 (2005).

[14] H.-T. Chen, W. J. Padilla, J. M. O. Zide, et. al. "Active terahertz metamaterial devices". *Nature* 444, 597-600 (2006).

[15] M. W. Klein, C. Enkrich, M. Wegener, et. al. "Second-harmonic generation from magnetic metamaterials". *Science* 313, 502-504 (2006).

[16] D. Huang, E. Poutrina, H. F. Zheng, et. al. "Design and experimental characterization of nonlinear metamaterials". *J. Opt. Soc. Am. B* 28, 2925-2930 (2011).

[17] M. K. Liu, H. Y. Hwang, H. Tao, et. al. "Terahertz-field-induced insulator-to-metal transition in vanadium dioxide metamaterial". *Nature* 487, 345-348 (2012).

[18] A. L. Rakhmanov, A. M. Zagoskin, S. Savel'ev, et. al. "Quantum metamaterials: Electromagnetic waves in a Josephson qubit line". *Phys. Rev. B* 77, 144507 (2008).

[19] H.-T. Chen, W. J. Padilla, M. J. Cich, et. al. "A metamaterial solid-state terahertz phase modulator". *Nat. Photon.* 3, 148-151 (2009).

[20] W. L. Chan, H. T. Chen, A. J. Taylor, et. al. "A spatial light modulator for terahertz beams". *Appl. Phys. Lett.* 94, 213511 (2009).

[21] N. I. Zheludev and Y. S. Kivshar. "From metamaterials to metadevices". *Nat. Mater.* 11, 917-924 (2012).

[22] H.-T. Chen, J. F. O'Hara, A. K. Azad, et. al. "Manipulation of terahertz radiation using metamaterials". *Laser Photon. Rev.* 5, 513-533 (2011).

[23] B. Ferguson and X. C. Zhang. "Materials for terahertz science and technology". *Nat. Mater.* 1, 26-33 (2002).

[24] G. P. Williams. "Filling the THz gap - high power sources and applications". *Rep. Prog. Phys.* 69, 301-326 (2006).

[25] N. I. Landy, S. Sajuyigbe, J. J. Mock, et. al. "Perfect metamaterial absorber". *Phys. Rev. Lett.* 100, 207402 (2008).

[26] H.-T. Chen, J. F. Zhou, J. F. O'Hara, et. al. "Antireflection coating using metamaterials and identification of its mechanism". *Phys. Rev. Lett.* 105, 073901 (2010).

[27] X. L. Liu, T. Starr, A. F. Starr, et. al. "Infrared spatial and frequency selective metamaterial with near-unity absorbance". *Phys. Rev. Lett.* 104, 207403 (2010).

[28] S. A. Kuznetsov, A. G. Paulish, A. V. Gelfand, et. al. "Matrix Structure of Metamaterial Absorbers for Multispectral Terahertz Imaging". *Prog. Electromagn. Res.* 122, 93-103 (2012).

[29] X. L. Liu, T. Tyler, T. Starr, et. al. "Taming the blackbody with infrared metamaterials as selective thermal emitters". *Phys. Rev. Lett.* 107, 045901 (2011).

[30] N. Liu, M. Mesch, T. Weiss, et. al. "Infrared perfect absorber and its application as plasmonic sensor". *Nano Lett.* 10, 2342-2348 (2010).

[31] C. H. Wu, B. Neuner, G. Shvets, et. al. "Large-area wide-angle spectrally selective plasmonic absorber". *Phys. Rev. B* 84, 075102 (2011).

[32] H. A. Atwater and A. Polman. "Plasmonics for improved photovoltaic devices". *Nat. Mater.* 9, 205-213 (2010).

[33] R. Alaee, C. Menzel, C. Rockstuhl, et. al. "Perfect absorbers on curved surfaces and their potential applications". *Opt. Express* 20, 18370-18376 (2012).

[34] K. Iwaszczuk, A. C. Strikwerda, K. B. Fan, et. al. "Flexible metamaterial absorbers for stealth applications at terahertz frequencies". *Opt. Express* 20, 635-643 (2012).

[35] C. M. Watts, X. L. Liu, and W. J. Padilla. "Metamaterial electromagnetic wave absorbers". *Adv. Mater.* 24, Op98-Op120 (2012).

[36] B. A. Munk. *Frequency Selective Surfaces: Theory and Design.* (John Wiley & Sons, New York, 2000).

[37] N. Engheta. "Thin absorbing screens using metamaterial surfaces". *IEEE Ant. Propagat. Soc. Internat. Symp.*, 2, 392 (2002).

[38] H. Tao, N. I. Landy, C. M. Bingham, et. al. "A metamaterial absorber for the terahertz regime: Design, fabrication and characterization". *Opt. Express* 16, 7181-7188 (2008).

[39] N. I. Landy, C. M. Bingham, T. Tyler, N. Jokerst, et. al. "Design, theory, and measurement of a polarization-insensitive absorber for terahertz imaging". *Phys. Rev. B* 79, 125104 (2009).

[40] D. Y. Shchegolkov, A. K. Azad, J. F. O'Hara, et. al. "Perfect subwavelength fishnetlike metamaterial-based film terahertz absorbers". *Phys. Rev. B* 82, 205117 (2010).

[41] J. Grant, Y. Ma, S. Saha, et. al. "Polarization insensitive terahertz metamaterial absorber". *Opt. Lett.* 36, 1524-1526 (2011).

[42] X. P. Shen, Y. Yang, Y. Z. Zang, et. al. "Triple-band terahertz metamaterial absorber: Design, experiment, and physical interpretation". *Appl. Phys. Lett.* 101, 154102 (2012).

[43] W. P. Qin, J. H. Wu, M. X. Yu, et. al. "Dual-band terahertz metamaterial absorbers using two types of conventional frequency selective surface elements". *THz Sci. Technol.* 5, 169-174 (2012).

[44] H. Tao, C. M. Bingham, A. C. Strikwerda, et. al. "Highly flexible wide angle of incidence terahertz metamaterial absorber: Design, fabrication, and characterization". *Phys. Rev. B* 78, 241103 (2008).

[45] M. Diem, T. Koschny, and C. M. Soukoulis. "Wide-angle perfect absorber/thermal emitter in the terahertz regime". *Phys. Rev. B* 79, 033101 (2009).

[46] Y. Yuan, C. Bingham, T. Tyler, et. al. "A dual-resonant terahertz metamaterial based on single-particle electric-field-coupled resonators". *Appl. Phys. Lett.* 93, 191110 (2008).

[47] H. Tao, C. M. Bingham, D. Pilon, et. al. "A dual band terahertz metamaterial absorber". *J. Phys. D Appl. Phys*

43, 225102 (2010).

[48] Q. Y. Wen, H. W. Zhang, Y. S. Xie, et. al. "Dual band terahertz metamaterial absorber: Design, fabrication, and characterization". *Appl. Phys. Lett.* 95, 241111 (2009).

[49] Y. Ma, Q. Chen, J. Grant, et. al. "A terahertz polarization insensitive dual band metamaterial absorber". *Opt. Lett.* 36, 945-947 (2011).

[50] L. Huang, D. Roy Chowdhury, S. Ramani, et. al. "Experimental demonstration of terahertz metamaterial absorbers with a broad and flat high absorption band". *Opt. Lett.* 37, 154-156 (2012).

[51] Y. Q. Ye, Y. Jin, and S. L. He. "Omnidirectional, polarization-insensitive and broadband thin absorber in the terahertz regime". *J. Opt. Soc. Am. B* 27, 498-504 (2010).

[52] J. Grant, Y. Ma, S. Saha, et. al. "Polarization insensitive, broadband terahertz metamaterial absorber". *Opt. Lett.* 36, 3476-3478 (2011).

[53] H.-T. Chen. "Interference theory of metamaterial perfect absorbers". *Opt. Express* 20, 7165-7172 (2012).

[54] L. Huang, D. Roy Chowdhury, S. Ramani, et. al. "Impact of resonator geometry and its coupling with ground plane on ultrathin metamaterial perfect absorbers". *Appl. Phys. Lett.* 101, 101102 (2012).

[55] J. F. O'Hara, E. Smirnova, A. K. Azad, et. al. "Effects of microstructure variations on macroscopic terahertz metafilm properties". *Act. Passive Electron. Compon.* 2007, Article ID 49691 (2007).

[56] Q. Y. Wen, Y. S. Xie, H. W. Zhang, et. al. "Transmission line model and fields analysis of metamaterial absorber in the terahertz band". *Opt. Express* 17, 20256-20265 (2009).